We are IntechOpen,
the world's leading publisher of
Open Access books
Built by scientists, for scientists

6,900
Open access books available

186,000
International authors and editors

200M
Downloads

154
Countries delivered to

Our authors are among the

TOP 1%
most cited scientists

12.2%
Contributors from top 500 universities

CLARIVATE ANALYTICS
BOOK CITATION INDEX
INDEXED

WEB OF SCIENCE™

Selection of our books indexed in the Book Citation Index
in Web of Science™ Core Collection (BKCI)

Interested in publishing with us?
Contact book.department@intechopen.com

Numbers displayed above are based on latest data collected.
For more information visit www.intechopen.com

Cooperative Control of
Multiple Biomimetic Robotic Fish

Junzhi Yu[1], Min Tan[1] and Long Wang[2]
[1] Lab. of Complex Systems and Intelligence Science, Institute of Automation
Chinese Academy of Sciences
[2] Department of Mechanics and Space Technologies, College of Engineering
Peking University
China

1. Introduction

There has been a spurt of interest in recent years in the area of group coordination and cooperative control among different research communities, involving biology, robotics, artificial intelligence, advanced control, sensor network, etc (Ögren et al., 2004; Kumar et al., 2005; Pettersen et al., 2006). As we know, fish shoals, bird flocks, etc exhibit typical aggregation behaviours, in which collective motions are employed to achieve useful tasks, e.g., avoiding predators, capturing prey, and breeding offspring. Similarly, when coordinating in unstructured or dynamic environments, it is possible that a team of relatively simple and cheap agents are capable of accomplishing complex tasks that exceed the capabilities of one single agent. In the robotic context, multi-robot systems presenting as distributed solutions have advantages such as increasing robustness to unexpected disturbances, fault-tolerance, thanks to redundancy, self-adaptation, and self-organization. Thus, applications of multi-robot systems are associated with a large group of autonomously functioning vehicles in the air, on land or sea or underwater, to jointly perform tasks such as demining operations, environmental surveillance, object transportation, search and rescue, and so forth (Kumar et al., 2002; Rabbath et al., 2007 ; Wang et al., 2007 ; Zhang et al., 2007).

Rapidly growing interests in cooperation and coordination of multi-robot systems have brought a lot of real-world applications as stated above. However, most significant efforts are devoted to ground and air based cooperation issues, and cooperative studies on underwater or surface vehicle are relatively few and immature (Rabbath et al., 2007). In particular, research on a group of robotic fish has not yet been implemented. The primary objective of this chapter is to build an artifical multi-fish system mimicking cooperative mechanism of fish flock, which provides a platform to test and verify the algorithms and strategies for cooperation of multiple underwater robots.

Although the topic of underwater biorobotics is not new, and there is a long history, the self-propelled, fish-like robots were indeed created in the 1990s (Triantafyllou & Triantafyllou, 1995; Triantafillou et al., 2004; Lauder et al., 2007a). The fish-like robot, i.e., robotic fish, as a marriage of biomechanism with engineering technology, is a cross-disciplinary subject

which mainly involves hydrodynamics based control and robotic technology. It is well known that fish have evolved to become the best swimmer in nature during millions of years' nature selection. They can easily achieve very high propulsive efficiency and maneuverability with little loss of stability through integrating multiple control surfaces including body, fins, and tail (Yu et al., 2004; Bandyopadhyay, 2005; Lauder et al., 2007a). As we expect, mimicking these biological systems will offer innovative, bio-inspired solutions to improving and even updating conventional underwater vehicles equipped with thrusters, which potentially bring increased performance in acceleration, speed, efficiency, maneuverability, stealth, etc (Sfakiotakis et al., 1999; Anderson & Chhabra, 2002; Triantafillou et al., 2004). Since the vast majority of the work to date on robotic fish has focused on the hydrodynamic mechanism of fish-like swimming, fish-like vehicles design, and control algorithms for fish-like locomotion, cooperative control of multiple robotic fish is surely an important subject for future real-world applications such as in military detection, undersea exploration, and management of water pollution. Moreover, the robotic fish based cooperation research will provide a useful reference for exploring the self-organizing mechanism of fish school, and understanding the collective behaviors by using only local information and interactions.

Despite fruitful work on cooperative control of multi-robot systems, most of these reference solutions can seldom be applied to the multi-fish system directly due to the unique locomotion mode of the robotic fish as well as the complex aquatic environment with many different sources of disturbance. Under such a dynamic environment, it is very difficult to design controllers that will guarantee system performance even in a local sense. So, the artificial multi-fish system, which is referred to as Multiple Robotic Fish cooperation System (MRFS), is established via behaviour-based approach. Specifically, using top-down design method, we propose a hierarchical architecture that comprises five levels: task level, role level, behavior level, action level, and controller level, to formalize the processes from task decomposition, role assignments, and control performance assessment. Furthermore, a vision-based closed-loop experimental system for multiple robotic fish is set up, where an improved parallel visual tracking method is formulated within a framework synthesizing features of fish features and surrounding disturbance. Since the robotic fish we employed have no ability of self-positioning, thus, an overhead, global vision subsystem is adopted to acquire information of the environment and the states of the fish. So our approach should be basically categorized into the centralized control. Then, rapid and accurate multi-fish tracking is crucial for decision-making. Currently, for the lab-based MRFS, a team of robotic fish (as large as eight) can perform some given tasks (primarily some challenging games) in a water tank with a dimension of 3.3 m × 2.3 m × 0.7 m (length × width × depth).

From a control engineering point of view, the MRFS can be considered as an integrated guidance packages that take into consideration the kinematics and the dynamics of the fish swimming, which functionally generates the motion commands for each fish. In this chapter, we provide a full development description for the MRFS, which is built on the basis of a series of free-swimming, radio-controlled, multi-link fish-like robots. There exist three salient features in MRFS:

- The custom-built fish-like robots are moderate sized, flexible, and easy to be controlled in a lab-based experiment configuration;
- The testbed is applicable to different cooperative tasks, and hence can be viewed a general one;

- High-level tasks within the hierarchical framework are ultimately decomposed into two primitive motion controllers, i.e., speed controller and orientation controller.

The rest of the chapter is organized as follows. An improved approach to design a multi-link robotic fish is outlined in Section 2. A vision-based subsystem to aid in identifying the fish and their surroundings is offered in Section 3. A hierarchical framework for coordinated control is presented in Section 4. The implementation of MRFS, including experimental results and discussions, are provided in Section 5 and Section 6. Section 7 contains the concluding remarks.

2. Design and Implementation of the robotic fish

In this section, we briefly present an overall design of a multi-link biomimetic fish prototype, describing its propulsive mechanism, mechatronic design, and motion control.

2.1 Multi-link based propulsive configuration

The rich variety of mechanisms employed by swimming organisms has long been an inspiration for biologists and engineers. Undulation of the axial structure, i.e., undulatory swimming, is the most general form of aquatic vertebrate locomotion. Regarding a fish as a hydrodynamic swimming machine, the central part of the fish body is support by jointed skeletal elements driven by muscle motors, while the tail acts as a propeller (Sfakiotakis et al., 1999; Lauder & Madden, 2007b). As we mentioned previously, self-propelled robotic fish capable of executing programmed motions not only provide a significant avenue for understanding locomotor questions in aquatic environment, but also enable estimating various conceptual designs for aquatic propulsion oriented robotic models. Attempts to replicate this delicate musculoskeletal structure are still not very successful. In general, there are two methods for designing fish-like propulsive mechanism in part (Yu et al., 2007). One is the hyperredundant, discrete body design, where a "multi-motor-multi-joint" structure is often adopted. Another is continuous body design, whose actuation is based on new-type smart materials such as polymers, elastomers and shape memory alloys, or on a special "single-motor-multi-joint" mechatronic layout. Because of the immaturity and delicacy of the continuous body design, the overall performance of the developed robotic fish is usually inferior to the discrete design scheme. With the purpose of developing a high-performance, self-propelled robotic fish with conventional actuation modes, we choose the multi-motor-multi-joint scheme. Particularly, the position-controlled servomotors are used to drive the multi-link fish. For more information on the continuous body design, the reader is referred to Bandyopadhyay (2004).

As biologists suggest, thrust is generated by momentum transfer to the surrounding water as a wave of bending passing down the deforming body during fish swimming. For convenience of describing these lateral body motions, strong emphases are laid on kinematic and anatomical data of vertebral column and tail. Typically, a propulsive wave form (hereafter referred to as body wave) that results from the progression of muscular contraction from head to tail is distilled to characterize the movement of the midline. Videler & Hess (1984) used a Fourier series to describe the body wave:

$$y_{body}(x,t) \simeq \sum_{j=1,3,5} \{a_j(x)\cos j\omega t + b_j(x)\sin j\omega t\} \tag{1}$$

where y_{body} represents the transverse displacement of the fish body, x denotes the displacement along the main axis, a_j and b_j denotes the Fourier coefficients derived from the digitized data. Barrett (1996) chose a propagating sine wave equation (2) as the reference body wave in the construction of a robotic tuna, which closely represents that of motion of a live tuna.

$$y_{body}(x,t) = (c_1 x + c_2 x^2)\sin(kx + \omega t) \qquad (2)$$

where k stands for the body wave number ($k=2\pi/\lambda$), λ is the body wave length, c_1 is the linear wave amplitude envelope, c_2 is the quadratic wave amplitude envelope, and ω is the body wave frequency ($\omega=2\pi f=2\pi/T$). Specially, like the Fourier coefficients a_j and b_j, the adjustable parameters c_1 and c_2 are choosen according to the collected data on realistic fish movements.
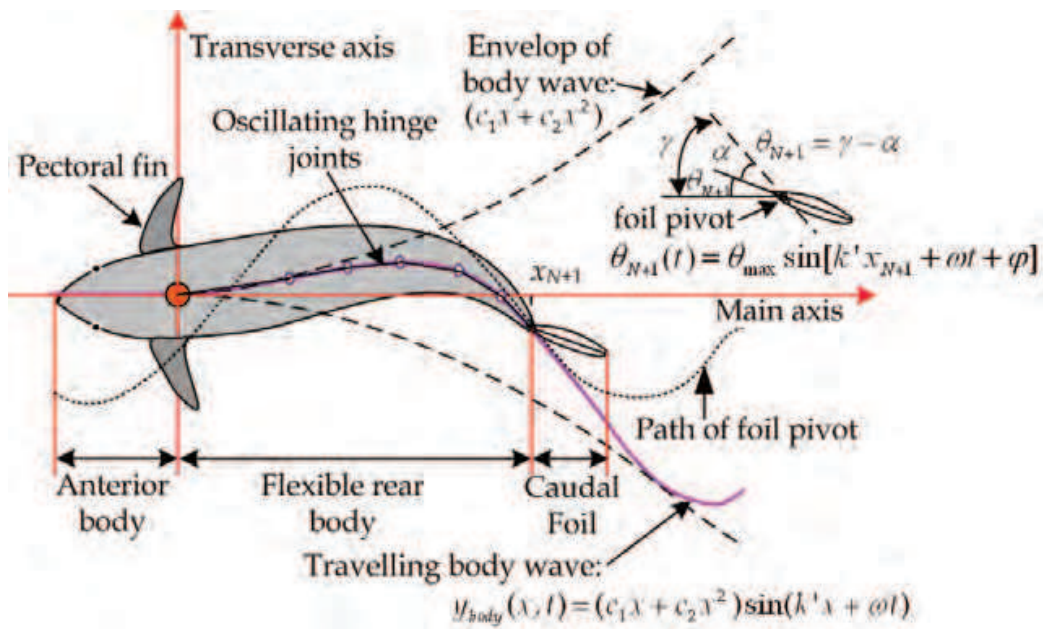

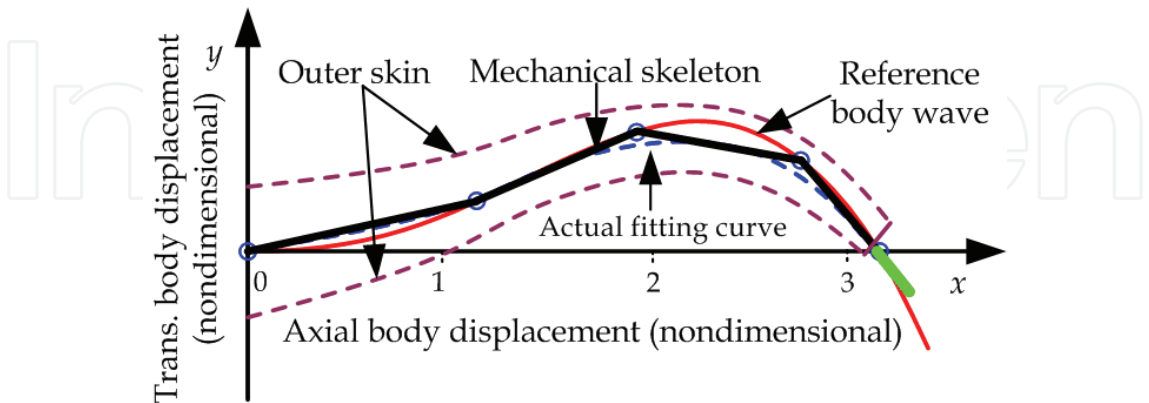Figure 1. A simplified propulsive model for a multi-link robotic fish

Figure 2. Actual fitting curve versus reference body wave in the multi-link robotic fish model

Fish is composed of tens of vertebra, as is observed, and each vertebra may be regarded as a miniature joint. The oscillatory part of the robotic fish, in this sense, could be discretely designed as a multi-link (or N-link) mechanism which consists of several oscillating hinge

joints actuated by motors. But it is hard to generate exactly a fish-like smooth wave with limited joints. How to use restricted joints to approximate the body waves exhibited in real fish is then a great challenge for robotics researchers. In our previous work, this problem is reduced to a numerical fitting issue of using a chain of links to approximate a discretized, spatial- and time-varying body wave (Fig. 1). During numerical operation, equation (2) is rewritten as (3) preserving the original body wave decomposed into two parts: the time-independent wave sequence $y_{body}(x, i)$ ($i = 0, 1, . . . ,M − 1$) in an oscillation cycle and the time-dependent oscillation frequency f which is regulated by the changing time interval between $y_{body}(x, i)$ and $y_{body}(x, i+1)$ when the robotic fish swims.

$$y_{body}(x,i) = (c_1 x + c_2 x^2)\sin(kx - \tfrac{2\pi}{M}i) \qquad i \in [0, M-1] \tag{3}$$

where i denotes the serial number in an oscillation cycle and M indicates the resolution of the discrete body wave. For more details of link-based body wave fitting we refer the reader to Yu et al. (2004).

In the above link-based body wave fitting, a precondition is imposed that the reference body wave (2) taken from the fast-swimming fish has an advantaged hydrodynamic and kinematic performance. We remark that this may not be true for various fishes in nature. When constructing a robotic prototype, a waterproof, outer skin is employed to envelop the multi-link based metal skeleton. The function of the elastic outer skin is to offer a smooth shape and reduce form drag. However, as shown in Fig. 2, an accompanying side effect that a relative difference between the actual fitting curve and the reference body wave arises after this elastic transition. In such a case, we can not ensure all points of link fall into the reference body wave in an oscillation cycle, but make each point in the multi-link move according to the reference body wave as closely as possible. Considering both ichthyologic characteristics and mechatronic constraints, an improved cyclic variable method is proposed to minimize the enveloped area between moving links and the reference body wave by searching the optimal link-length ratio ($l_1 : l_2 : . . . : l_N$). The comparative results, before and after the optimization, have partly demonstrated satisfactory performance of this link-length ratio optimization in forward locomotion, turning maneuvers, and energy savings. The optimal link-length ratios for three-link and four-link robots are 1 : 0.72 : 0.65 and 1 : 0.73 : 0.63 : 0.61, respectively, which are applied to later robotic prototypes. More detailed geometric optimization of relative link lengths for robotic fish can be found in Yu et al. (2007).

Besides multi-link flexible fish body, another fundamental design feature is caudal fin for a fish propelled by body surface and caudal fin. In the artificial fish system, the rigid anterior body is mechanically connected to the front of the multi-link flexible fish body, while the caudal fin is fixed to the lattermost link. The attached caudal fin rotates around the fin pivot in a sinusoidal fashion taking the form of equation (4).

$$\theta_{N+1}(t) = \theta_{\max}\sin(kx_{N+1} + \omega t + \varphi) \tag{4}$$

where $\theta_{N+1}(t)$ indicates the pitch angle of the caudal fin with respect to the main axis, θ_{max} the amplitude of the pitch angle, φ the phase angle between the heave and the pitch, and x_{N+1} the x-component of the position of the moving foil pivot. As a practical way, θ_{max} can be calculated as:

$$\theta_{\max} = \gamma_0 - \alpha_0 = \arctan(\frac{\partial y}{\partial x}(x_{N+1}\mid_{y_{N+1}=0},t)) - \alpha_0 \tag{5}$$

where γ_0 denotes the angle corresponding to the slope of $y_{body}(x_{N+1},t)$ at $y_{N+1}=0$, and a_0 is the angle of attack of the caudal fin at $y_{N+1}=0$.

As summarized in Yu et al. (2005), of the most prominent characteristics associated with fish-like robots, there are four parameters that constrain the swimming performance:

- The first one is the length ratio of the fish's oscillatory part to the whole body, R_l ($0 < R_l \leq 1$). The fish will switch from a carangiform swimmer to an anguilliform one relying on different values of R_l. With the decrease of R_l, in general, the efficiency and speed of fish swimming remarkably increase, but the maneuverability reduces to a certain extent.
- The second one is the number of simplified joints (segments) in oscillatory part, N. Larger value of N, in principle, will lead to better maneuverability and redundancy, but harder construction and control of the robot.
- The third one is the link-length ratio of links in the oscillatory part, $l_1 : l_2 : \ldots : l_N$. The length of each link in the direction from nose to tail, generally speaking, is getting smaller and smaller. The oscillatory amplitude, in contrast, increases gradually and reaches its maximum at the tail peduncle of the fish.
- The last one is the shape of the caudal fin.

Taking a further step towards capturing key features of the functional design of fishes, we have developed a custom-built executive routine DFS (Digital Fish Simulation). This fish-oriented simulation platform integrating the geometric optimization of relative link lengths, is based on a WINDOWS XP operation system with a compiler of Microsoft Visual C++ 6.0. A snapshot of this execution is illustrated in Fig. 3. It mainly consists of four components: theoretical calculation, body wave configuration, curve generator, and animation. Friendly Graphical User Interface (GUI), coupled with the ability to partly mimic the kinematics and hydrodynamics of locomotion in vivo, supplies a powerful tool for understanding key points in fish based propulsion and for preliminary assessment of fish-like robotic schemes.
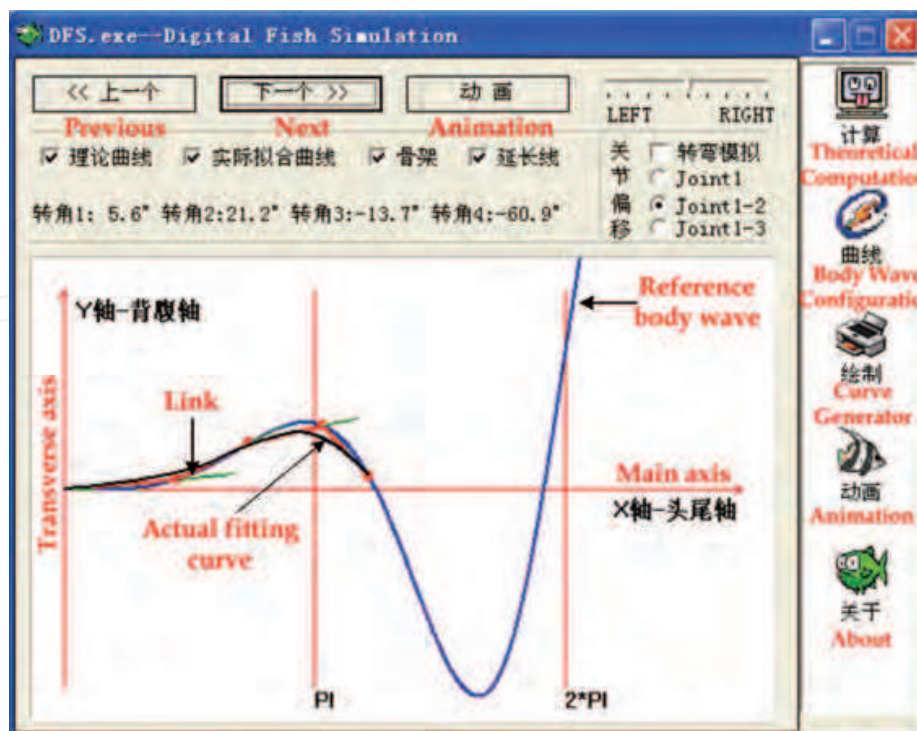

Figure 3. A snapshot of the Digital Fish Simulation platform

2.2 Mechatronic implementation of robotic fish

The fish-like devices, as addressed previously, have a huge potential for precise control of kinematics and non-biological parameters validation, which provides a self-contained test bed for designing bio-inspired underwater vehicles. A series of radio-controlled, self-propelled robotic fish, based on the simplified propulsive mechanism after optimization, have been developed. The mechanical configuration for a four-link robotic fish capable of up-down movement via a pair of artificial pectoral fins is illustrated in Fig. 4, and its drive and control architecture in Fig. 5. It can swim realistically like a fish in the water tank. Fig. 6 exhibits six types of fish-like robots, which are primarily consist of six parts:

- **Support unit** (aluminum exoskeleton + head + anterior body)
- **Actuator unit** (DC servomotors)
- **Sensor unit** (infrared, visual, ultrasonic, etc)
- **Communication unit** (wireless receiver)
- **Control unit** (microprocessor + peripherals)
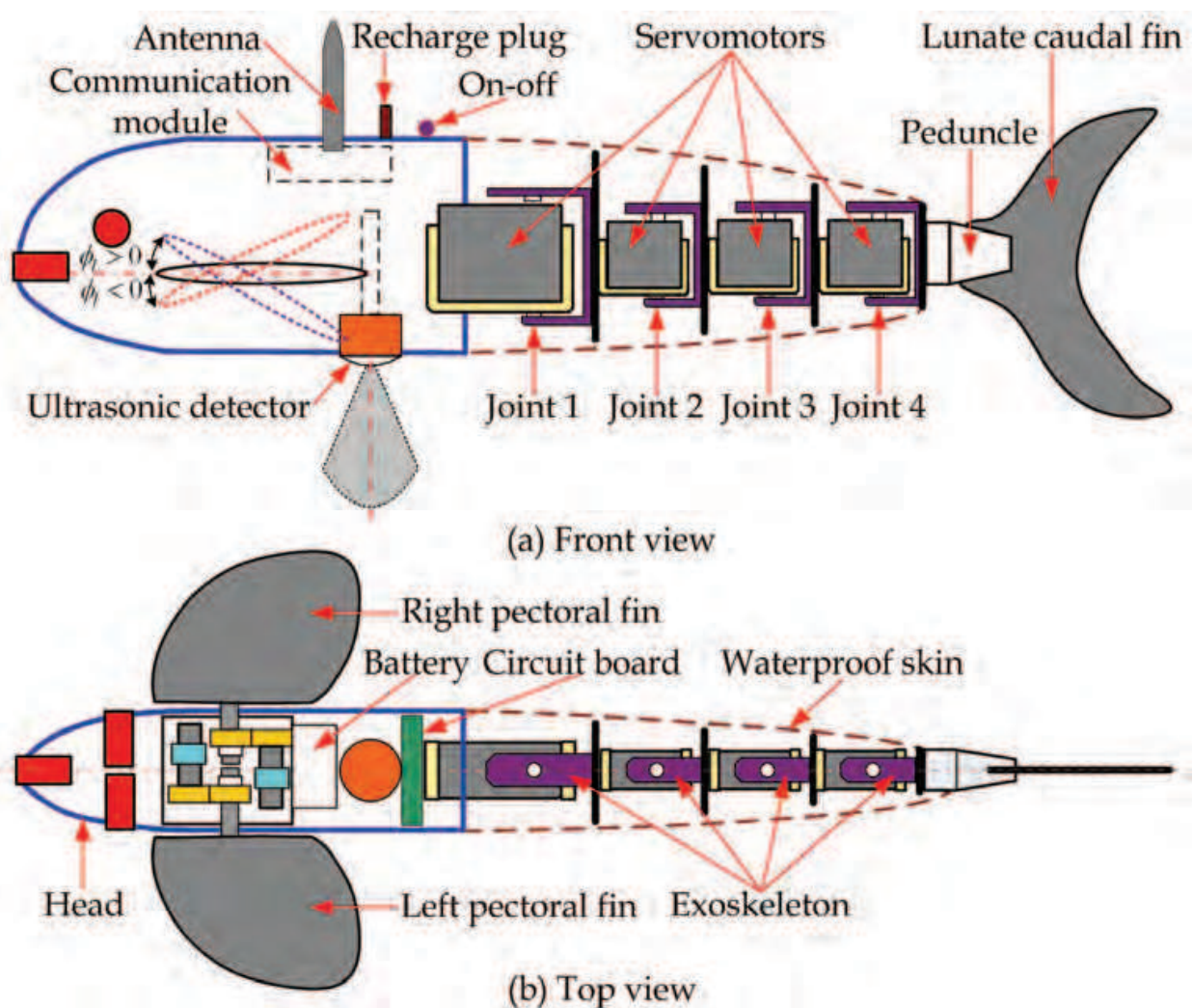- **Accessories** (batteries, waterproof skin, tail fin, etc)

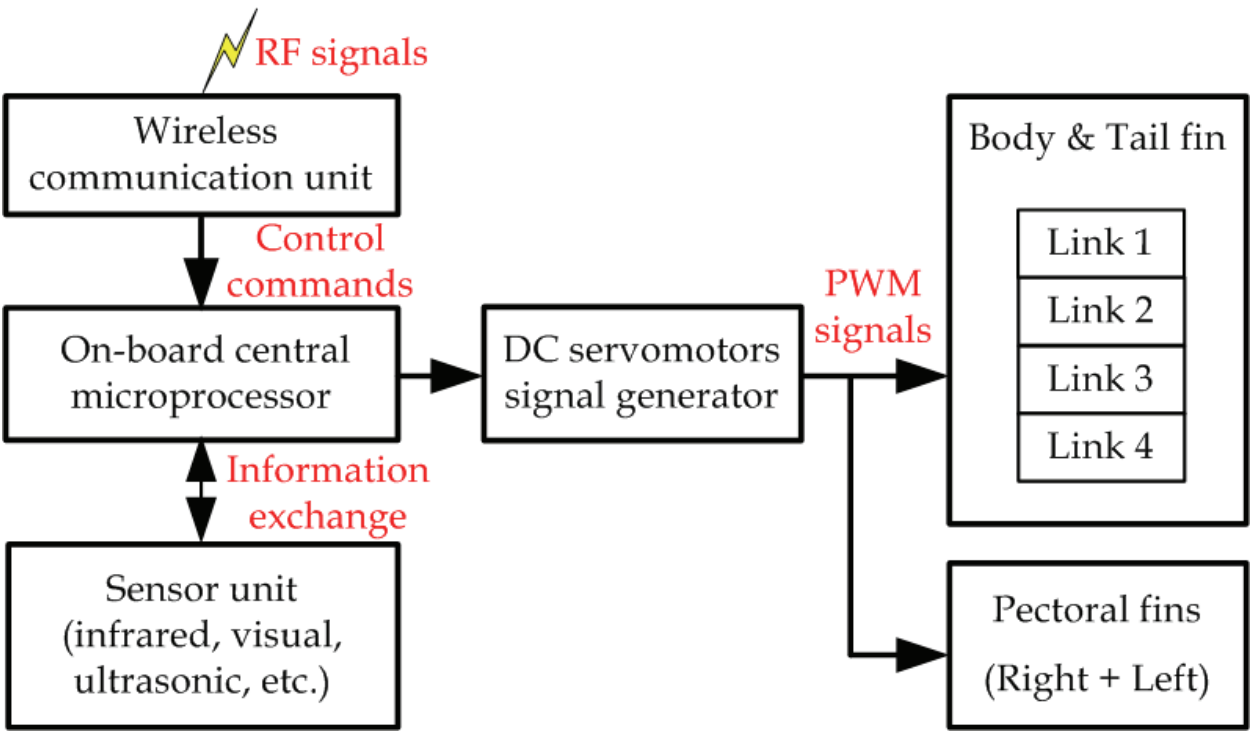Figure 4. Mechanical structure of the multi-link robotic fish with a pair of pectoral fins

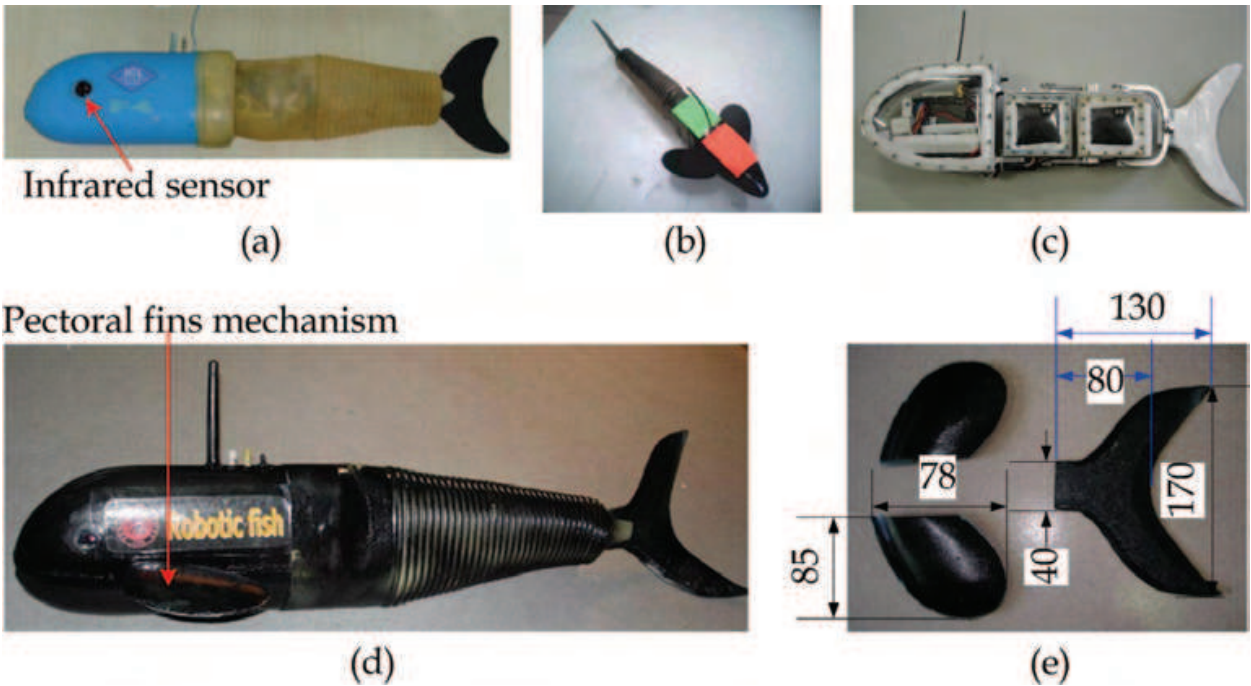Figure 5. Architecture of the actuator and control units

Figure 6. Prototypes of different robotic fish. (a) Four-link robotic fish equipped with infrared sensors, 405 mm in length; (b) three-link robotic fish, 380 mm in length; (c) two-module, reconfigurable robotic fish; (d) four-link, multimode robotic fish with the capability of autonomous three-dimensional (3-D) swimming, 650 mm in length; (e) shape and dimension of both pectoral and caudal fins of the multimode fish

For a lab-based purpose, the fish head and anterior body are united as a streamlined hull which is molded using fiberglass. The hollow head offers a considerable space to amount

the control unit, communication unit, sensor unit, mechanical pectoral fins, and batteries. The rear body is composed of multiple links actuated by DC servomotors, which actively performs lateral fish-like oscillations. Notice that the mechanical arrangement of the oscillatory links is referred to the optimized $l_1 : l_2 : \ldots : l_N$. The links are further externally connected by a lightweight exoskeleton, whose outside is wrapped by an impermeable but stretching skin. Meanwhile, a partly flexible lunate foil connected to the last link acts as the caudal fin. Taking into account that the swimming performance of the robot depends upon the material property of the tail fin to some degree, we adopt rubber to achieve chordwise and spanwise flexibility of the tail fin. Some extensible units, for an advanced version, can be integrated. For instance, three infrared sensors located at the front, the left, and the right of the anterior part of the robotic fish as shown in Fig. 6(a), are used to avoid obstacles autonomously during forward swimming, whereas an ultrasonic detector (510 kHz) located at the bottom of the head is utilized to measure the vertical distance between the fish and the floor of testing water tank. Also, a pair of mechanical pectoral fins (see Fig. 6(d)) whose actuation (DC servomotor) and control are independent of each other, are used for diving/climbing in the vertical plane. Specifically, the shape and dimension for both pectoral and caudal fins are illustrated in Fig. 6(e). Moreover, to ensure a reasonable balance between the resultant gravitational forces and buoyant forces, i.e., to achieve an approximately neutral buoyancy state, some balance weights may empirically be added to or removed from the lower side of the head and exoskeleton. For a large-scale robotic fish, an automatic adjustment mechanism can be fixed to achieve this end.

Two control modes, to date, have been developed: the manual control mode via a remote controller and the automatic control mode via a closed control loop through wireless communication. Table 1 presents basic technical parameters of the robot shown in Fig. 6(a). At this stage, without fish-based 3-D self-positioning ability, a free-swimming robotic fish enabling two-dimensional (2-D) steady swimming and turning maneuvers is chosen as the subject of cooperative control.

Items	Characteristics
Dimension (L × W × H)	~ 405 mm × 55 mm × 88 mm
Weight	~1.38 kg
Sensor	3 infrared sensors (front + left + right)
Number of the links	4
Length of the oscillatory part	~ 200 mm
Maximum forward speed	~ 0.42 mm
Minimum turning radius	~ 200 mm
Actuator mode	DC servomotor
Maximum input torque	3.2 kg.cm
Control mode	RF (433 Hz)
Working volt	4.8 V

Table 1. Technical parameters of a self-propelled, four-link robotic fish

2.3 Motion control

The conspicuous hallmark of fish-like swimming is the compound propulsive system that integrates the maneuvering hardware into the propulsion hardware. Due to this particular

propulsion mode, plus the complexity of the water environment, there exist several difficulties in controlling a robotic fish flexibly and robustly, which are listed as follows:

- Firstly, it is very difficult to establish a precise mathematical model for fish-like swimming via purely analytical methods, since how fish generate forces and maintain stability during propulsion and maneuvering is not well understood. So we can only predict approximately the response of the robot after the control commands are sent.
- Secondly, the robotic fish hardly track a straight line because of inherent lateral oscillation fashion. That is, the movement of a robotic fish is essentially nonlinear, and its swimming pattern is changing dynamically.
- Thirdly, the fish cannot move reversely like a wheel-like mobile robot during propulsion.
- Lastly, waves will be produced when a robotic fish moves. In this case, the movement of the robotic fish will be affected by the waves no matter they are in a stable state or not. This further leads to the uncertainty of the sensory information and the imprecise localization control.

To confront such challenge, we assume that the controllability of the fish relies on the internal shape (the joint angle ϕ_{ij}) for maneuverability and the oscillating frequency f of the moving links for speed. More specifically, the simplified propulsive model presented in Section 2.1, which relates frequency to speed and joint angle bias to turns, is used to generate a variety of swimming patterns. Then the motion control problem in the 2-D plane is decomposed into the speed control and the orientation control. Furthermore, for a robotic fish capable of up-and-down movements, in particular, submerging/ascending control has to be implemented in the 3-D workspace. For instance, the robotic fish is able to execute 3-D motion by adjusting the attack angle of the pectoral fins like sharks that do not have swim bladders.
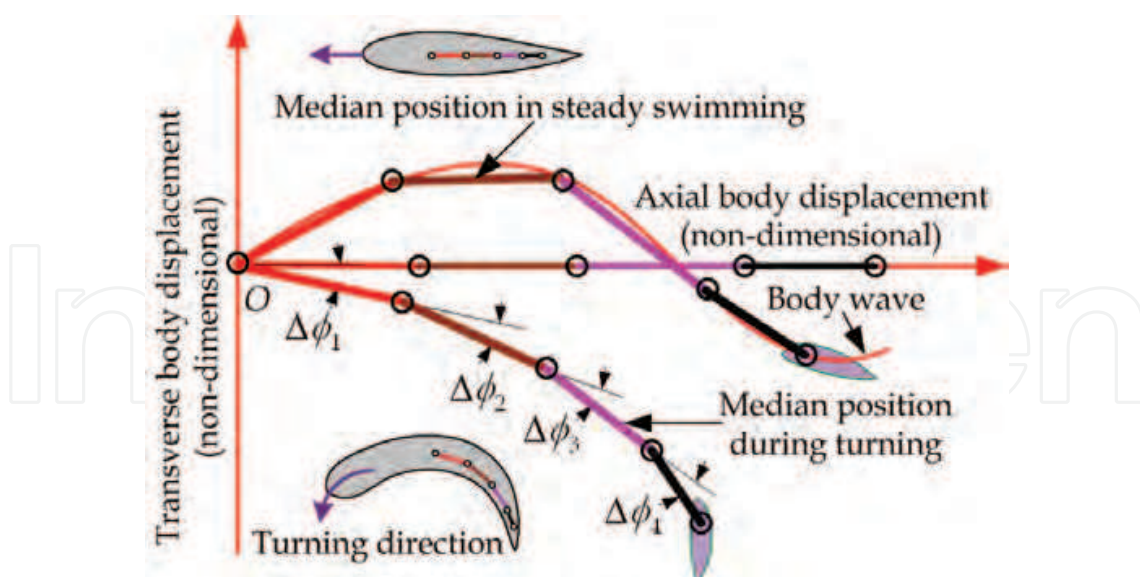

Figure 7. Schematic diagram of adding deflections to the oscillatory links enabling turning maneuvers

As for the speed control, there are three basic approaches to achieve different swimming speeds.

- **Speed control based on the oscillating frequency *f*.** As a general tendency, the advancing speed increases with increasing *f*, and *f* will approximate a constant when the desired speed is arrived.
- **Speed control based on the oscillatory amplitude.** A second order amplitude envelop $(c_1 x + c_2 x^2)$ is applied to produce different body waves through different values of c_1 and c_2, as shown in (2). In practice, oscillatory-amplitude based speed control method can generate different speeds when *f* is fixed.
- **Speed control based on the length of the oscillatory part.** As stated previously, R_l is a vital characteristic parameter, and not all the body or the oscillatory portion contributes to thrust generation at all time, it may be a feasible way to employ different lengths of the oscillatory part at various speeds. For a multi-link robotic fish, this method can be easily operated by locking or unlocking some links. Therefore, the robotic fish can switch between the anguilliform mode and the carangiform one so as to achieve various motions and better swimming performance.

With respect to varying the swimming directions, we add different deflections (i.e., dynamic offsets) to the straight, symmetric gaits propelled only by an oscillating posterior body and tail fin to accomplish various turns. That is, the flexible posterior body and tail moving in the form of body wave is forcibly deflexed to ensure an asymmetric motion, which provides large lateral forces for maneuvering (Read et al., 2003). As depicted in Fig. 7, an internally asymmetric shape of the robot can geometrically be yielded via adding different deflections $\Delta\phi_j$ to each joint. A 2-D array Ctrl_Data[*M*][*N*] (6) for the joint angles can eventually be calculated according to the link-based fitting method (Yu et al., 2004), where $\Delta\phi_j$ is the joint angle between the *j*th link and the (*j* − 1)th link at the interval of the *i*th (*i* = 0, 1, . . . , *M* − 1) link, satisfying $\phi_j = \theta_j - \theta_{j-1}$. Practically, Ctrl_Data[*M*][*N*] is saved as a lookup table stored in the nonvolatile electrically erasable programmable read-only memory (EEPROM) of microcontroller, which serves as the primitive control data for steady swimming and turning maneuvers.

$$\text{Ctrl\_Data}[M][N] = \begin{pmatrix} \phi_{01} + \Delta\phi_1 & \phi_{02} + \Delta\phi_2 & ... & \phi_{0,N} + \Delta\phi_N \\ \phi_{11} + \Delta\phi_1 & \phi_{12} + \Delta\phi_2 & ... & \phi_{1,N} + \Delta\phi_N \\ ... & ... & ... & ... \\ \phi_{M-1,1} + \Delta\phi_1 & \phi_{M-1,2} + \Delta\phi_2 & ... & \phi_{M-1,N} + \Delta\phi_N \end{pmatrix} \tag{6}$$

For a given turning maneuver, in addition, it can theoretically be achieved by governing magnitude, position, and time of the deflections applied to the moving links. Since the turning maneuver can mathematically be triggered by multiplying a smoothed step function $u(t, \beta, t_0)$ to deflection angle $\Delta\phi_j$, we can then unify different turning maneuvers into a framework by choosing suitable step-function combinations $\sum \varpi_{j'} \mu(t, \beta, t_{j'})$ and $\Delta\phi_j$ (Yu et al., 2006a).

$$\mu(t, \beta, t_0) = \frac{\text{atan}(\beta(t - t_0)) + \arctan(\beta t_0)}{(\pi / 2) + \text{atan}(\beta t_0)} \tag{7}$$

where β denotes the positive rise coefficient, t_0 indicates the initial rise moment, *j* is the *j*'th directed (i.e., positive or negative) width coefficient, and $t_{j'}$ is the *j*'th rise moment (*j*' = 0, 1, .

. ., N' and N' is a positive integer). For example, when a deflection of $\sum \varpi_{j'} \mu(t,\beta,t_{j'}) \times 45°$ is applied to the first two joints of the flexible rear body, a simulated trajectory (Fig. 8) in which the robot can avoid the obstacle successfully is produced. The key to such a relatively complicated maneuver is to decide the suitable $\sum \varpi_{j'} \mu(t,\beta,t_{j'}) \times \Delta\phi_j$, where $\sum \varpi_{j'} \mu(t,\beta,t_{j'})$ takes a form of (8) plotted as Fig. 9.

$$\sum \varpi_{j'} \mu(t,\beta,t_{j'}) = \mu(t,\beta,t_0) - 2 \times \mu(t,\beta,t_1) + 2 \times \mu(t,\beta,t_2) - \mu(t,B,t_3) \tag{8}$$
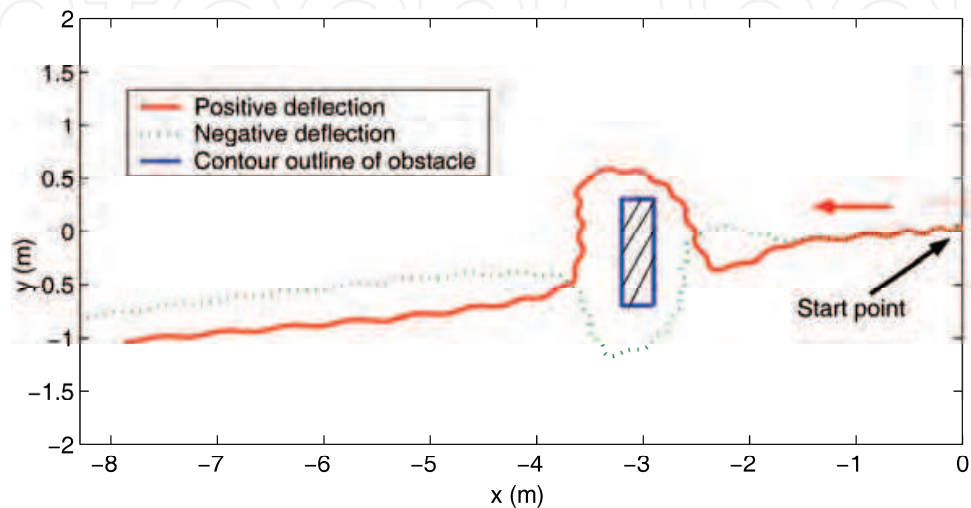
Figure 8. Simulated trajectory for a simple obstacle-avoidance case
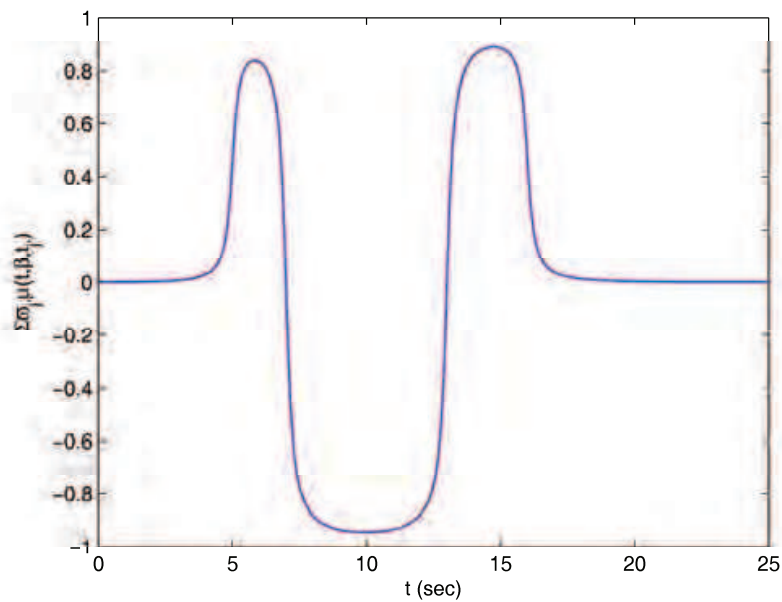
Figure 9. Graphical description of the step-function combination applied to an obstacle-avoidance case

As can be observed from Fig. 9, when the robotic fish swims without turning, $\sum \varpi_{j'} \mu(t,\beta,t_{j'}) \times \Delta\phi_j = 0$, else $\sum \varpi_{j'} \mu(t,\beta,t_{j'}) \times \Delta\phi_j \neq 0$. More specifically, $\sum \varpi_{j'} \mu(t,\beta,t_{j'})$

decides the moment of performing turning while $\Delta\phi_j$ is responsible for turning magnitude (i.e., turning diameter). So, we can infer that $t_0 \neq 0$ holds in the case of *turning during advancing*, that $t_0 = 0$ in the *turning from rest*, and that $\left|\Delta\phi_j\right| = \Delta\phi_{\max}$ in the *snap turning*, which corresponds to three basic turning modes defined by Yu et al. (2004). Naturally, some primitive swimming gaits: *straight cruising*, *turn left*, *turn right*, *braking*, etc, can be further devised.

Additionally, some task-oriented swimming modes are designed besides above-mentioned bio-inspired gaits. For instance, pushing an object (e.g., ball) exactly is beyond the natural swimming modes for a fish, but we can define such an artificial swimming mode. Fig. 10 depicts a video sequence of pushing ball, which is entirely composed of a series of primitive swimming modes: *straight cruising*, *turning during advance*, *snap turning*, etc.

To satisfy the demand of real time in cooperative control, we further adopt a PID controller for piecewise speed control and a fuzzy logic controller (FLC) for orientation control, which are presented particularly in our previous work of Yu et al. (2004).
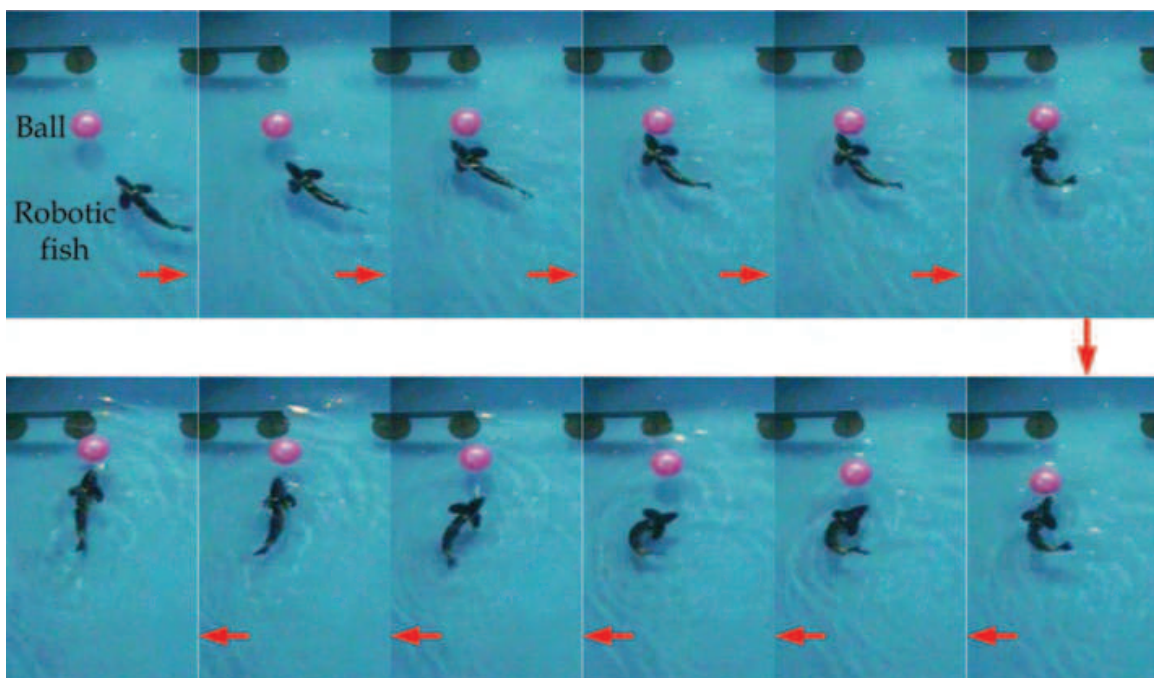

Figure 10. A continuous sequence of pushing ball

3. Visual tracking of multiple robotic fish for cooperative control

The aim of this section is to solve the problem of visual tracking of multiple robotic fish (as large as eight) for cooperative control, where a team of robotic fish in a larger tank by 3.3 m × 2.3 m × 0.7 m are required to perform some given tasks. Since the robotic fish we employed have no ability of self-positioning, thus, an overhead, global vision subsystem is adopted to acquire information of the environment and the states of the fish. As we know, if images are processed more quickly, decisions will be made more efficiently in a control cycle. Hence fast and accurate multi-fish tracking is a central issue for cooperation based decision-making.

For our testing, a CCD camera with wide view which is hung perpendicularly above the water tank (about 2.6 m high) is responsible for capturing the environment information, and the motion status information of the robotic fish within an area of 3.3 m × 2.3 m. The output of the camera is directly fed into a video digitizing card. The sampled resolution is 520 × 384 pixels for each frame, which frame processing rate holds 25 Hz. Unlike conventional ground-based identification, the robots work underwater and flex their body to move, which induces surface waves and even splashes. Moreover, a small quantity of colors less than six can robustly be identified in the laboratory environment, failing to meet the cooperative demand of as large as eight robots. To cope with this situation, anti-jamming measures including optical correction and foil superposition are firstly pre-implemented before segmentation. A color-based thresholding combined with binary coding is then adopted to binarize the sampled image, and a color-index based identification to distinguish the moving fish (Yu et al. 2003; Yu et al. 2006b).

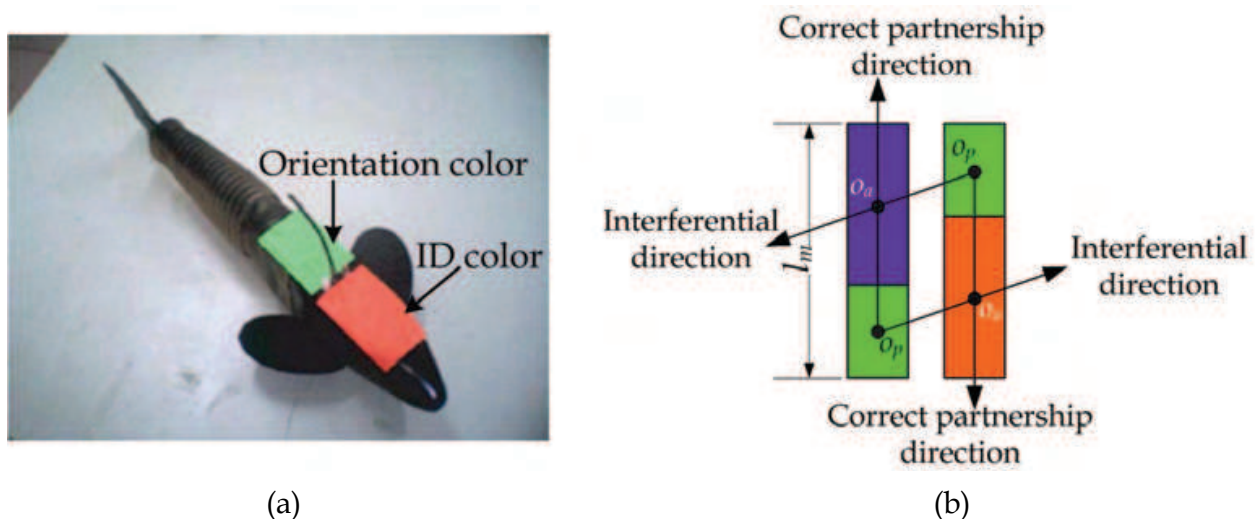(a)   (b)

Figure 11. Scheme of color identification. (a) A robotic prototype attached a color mark; (b) schematic of the color mark

Fig. 11 illustrates a robotic prototype with a custom-built color mark composed of ID color and Orientation color. The robotic fish, as an elongate body, allows a short and narrow space for attaching the color mark. Naturally, two small, different color marks are employed to yield necessary position and orientation information of the fish, i.e., to calculate the centroid and the slope of the color block. Based on this heuristic scheme (Yu et al., 2003), suppose that the number of the colors that can be recognized clearly in various underwater conditions is Q, the vision system will accommodate at most $Q - 1$ robotic fish, where Q stands for a positive integer not less than two. However, experiments show $Q = 6$ for our lab-based lighting. So we can only identify five fish using this scheme, which may not satisfy the demand of at most eight robotic fish to be positioned in MRFS. After analysis, we find the orientation color is not used sufficiently in this scheme. As a remedy, available colors are uniformly arranged in two groups: anterior color group and posterior color group. Making a permutation and combination for the two groups, there is a sum of $int(Q/2) \times int(Q/2)$ to be theoretically distinguished, where $int( )$ denotes the integer function. Note that we are able to identify nine (3 × 3) fish with this scheme. The next task is how to work out this scheme considering all possible cases occurred in testing.

As shown in Fig. 11b, the anterior color block is aligned with the posterior block, and the orientation of the mark is prescribed as the centroid of the posterior block (o_p) directs towards the anterior one (o_a). A sticking point in this scheme is to precisely recognize partner of the anterior block. Empirically, we search the recorded centroid within a circular area, whose center coincides with the o_a and radius is chosen as $2l_m/3$, where l_m is the total longitudinal length of the anterior block plus the posterior one. In most cases, only one o_p can be found, which means the anterior block has successfully been matched its partner. A tag is simultaneously attached to globally declare its state. However, an unfavorable case would arise, in which two marks are too close and two posterior centroids can be found. To deal with this situation, like the heuristic mark identification method, we have to calculate the longitudinal centerline of the anterior block by a least square fitting so as to offer assistance in judging the right posterior partner. After all, there seems to be little probability of triggering this extreme condition.
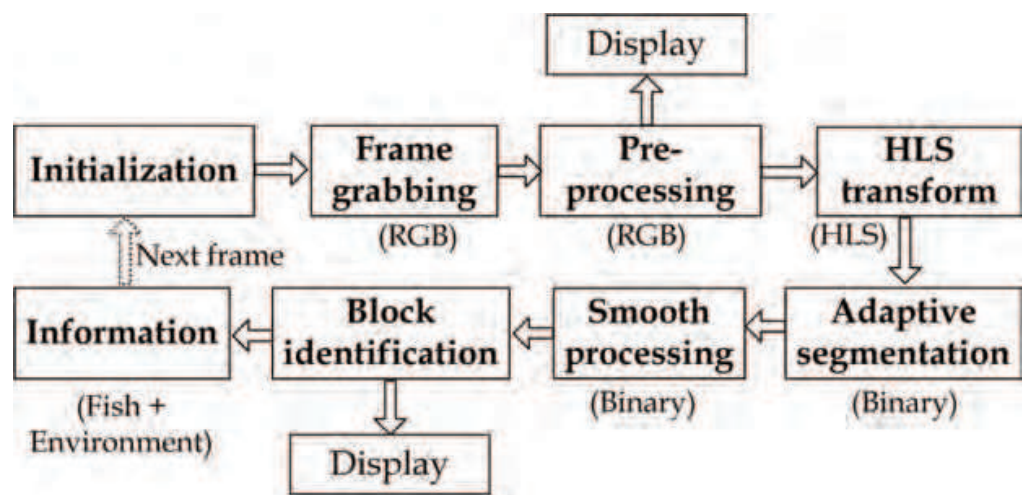

Figure 12. Block diagram of an overall multi-fish tracking procedure

To speed up locating interested pixels during adaptive segmentation and closure operation, all time-consuming, iterative image operations are optimized with the aid of parallelized SIMD (single-instruction, multiple-data) technologies embedded in processors. Fig. 12 summarizes the overall tracking operations in block diagram. Following a sequence of frame grabbing, pre-processing, HLS transform, adaptive segmention, smooth processing, identification, and information output, we can obtain the desired information on the multi-fish and their surroundings, which is served as a basis for effective decision-making. To reduce adverse disturbance resulting from capture hardware and illumination change, a pre-processing involving optical correction and foil superposition is conducted before the image segmentation. Also note that the sampled video in 24-bit RGB is converted to widely used HLS color space through HLS transform. This is because R, G, and B components of image data are scattered and correlated, rendering malfunction in most visual applications.

To further evaluate the performance of multi-fish tracking, strict tests are executed on a WINDOWS XP operation system with a Pentium IV 3.0 G processor, a memory of 1 G, and a compiler of Microsoft Visual Studio.net 2003. When the resolution disposed is set to 624×434 pixels in 24 bits, high-precision functions, *QueryPerformanceFrequency()* and *QueryPerformanceCounter()*, which are embedded in the operation system, are employed to measure the runtime of a processing cycle. In a static environment with projected lamplight, it only takes about 24.143 ms to identify eight fish marks and an obstacle demonstrated in

Fig. 13 in one cycle, compared with 167.893 ms coded in C++ Language. The speedup ratio is as high as 6.9. Meanwhile, a typical update rate for the frame grabbing is 40 ms allowing plenty of time for cooperative algorithms and other operations.
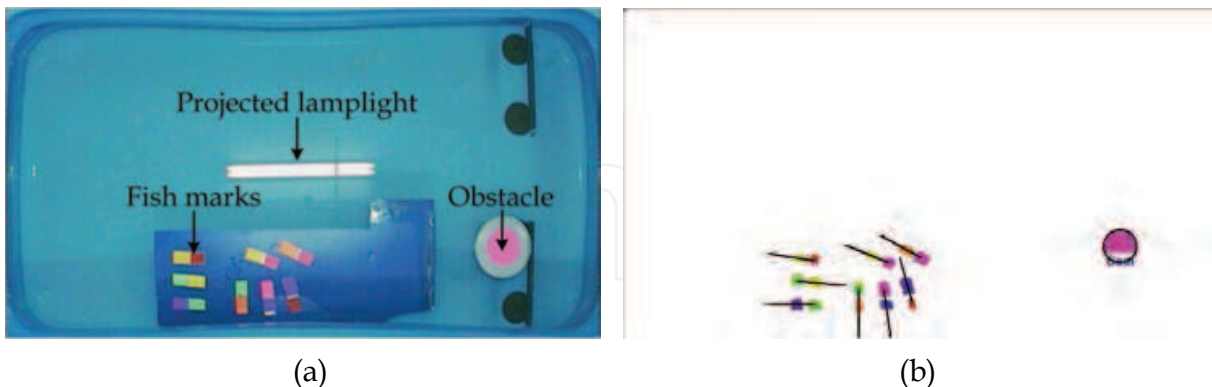

(a)   (b)

Figure 13. Experimental scenario and results of multi-object tracking. (a) Eight fish marks and an obstacle floating on the water tank; (b) identification results associated with positions and moving direction

4. Hierarchical architecture for cooperative applications

In this section, we propose a hierarchical control algorithm for cooperative applications in MRFS. A five-level hierarchical architecture is illustrated in Fig. 14.

The first level is task planner level. In this level, a coordinator is designed to acquire and, more importantly, to process the vision information involving the fluid circumstance and the states of robotic fish. Therein, the kinematics of the fish contained in the sampled image can be extracted by analyzing moving marks in real time. The required task is then decomposed into different roles on the basis of global, vision-derived information. A prediction should be ensured that these roles are competent for the assigned subtask during the decomposition.

After producing different roles, we concentrate on the role assignments which are executed in the second level. Since any fish member has the same capabilities and can take on any role within the task, we should select the most qualified candidate for each role according to some appropriate rules and try to achieve the task effectively as a whole. To confront with specific requirements for different tasks, we introduce both static and dynamic role assignments mechanism. For static assignments, once roles are decided at the beginning of the task, they will not shift during the implementation of the tasks. But for the dynamic assignments mechanism, the fish may switch their roles according to the progress of the task.

The third level is the behavior level, in which different component behaviors are designed for each role. In this level, protocols in the form of finite state automaton (FSA) are employed to organize these behaviors, formalizing the switches and restraints between them. In practice, the design of behaviors, bio-inspired or artifical, has a great impact on the efficiency and performance of cooperative control. Note that the robotic behaviors and roles are designed to be complementary to each other, so that a fish group exhibiting good collective behavior can be achieved.

Following the behavior level is the action level, in which a sequence of actions is assembled for a specific behavior. Considering the fluid circumstance and mechanical constrains of the fish body, five basic actions are designed, which are *turning during advancing*, *snap turning*, *turning from rest*, *forward advancing*, and *drifting*. The first three actions may be further

divided into two categories: *turn to right* and *turn to left*. More advanced behaviors such as obstacle avoidance, moving to goal, and wander can be achieved by combining these basic actions in a certain sequence.

The last level, which is called the controller level, is the lowest one. As mentioned above, the fish's motion control, that is action control, can ultimately be resolved into two parallel types of control laws: the speed controller and the orientation controller. Given a desired speed, a PID controller is applied. Meanwhile, a fuzzy logic controller is imported as a solution to the orientation control.
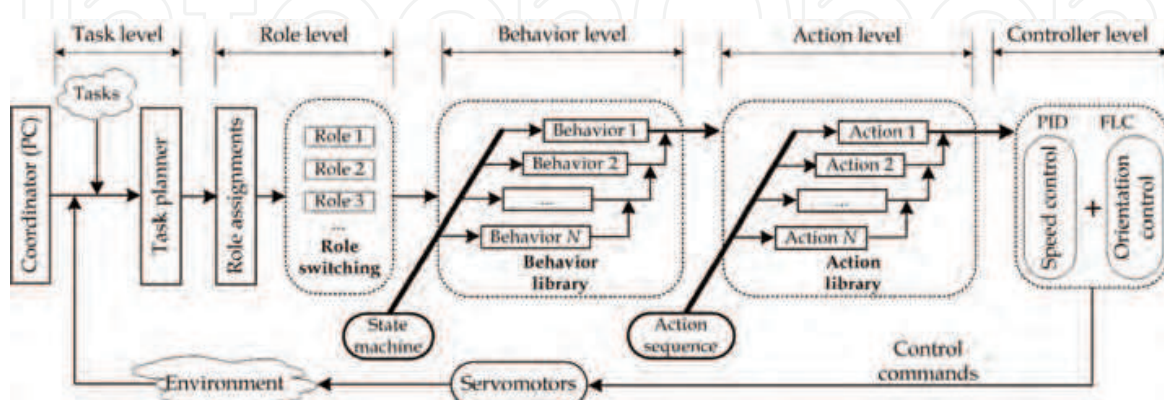
Figure 14. Block diagram of a hierarchical architecture for cooperative control

5. Design and implementation of the MRFS platform

For the sake of investigating fish-like propulsion and underwater robots based cooperative control, we have developed an experimental platform MRFS shown in Fig. 15. The hardware platform can roughly be decomposed into four subsystems: robotic fish subsystem, visual tracking subsystem, decision-making subsystem, and wireless communication subsystem. The robotic fish, as the executors, swim in the tank and implement control commands generated from the host computer. The information about the fish and their environments which are marked with specified colors in the experiments, are captured by an overhead camera with wide view. The camera is directly connected to the frame grabber embedded in the computer, and the captured information is sent to the computer in real time. After the image information is effectively processed in the visual tracking subsystem, they are sent to the decision-making subsystem as inputs. Then, based upon input signals and specific control strategies for given tasks, the decision-making subsystem generates corresponding control commands and transits them to each fish through the wireless communication subsystem. Thus, a full control loop is implemented.

A task-oriented software platform that is compatible to the hardware architecture is further developed. This software incorporates visual tracking, cooperative control, and bidirectional communications, on which users can perform multifold functions related to task selection, parameter setting, image processing, control algorithms loading, as well as real-time display. Fig. 16 depicts the well-designed graphical user interface (GUI) for MRFS. This GUI, from the perspective of function, can be divided into the following six components:

- **Real-time display**, where the globally captured image covering the overall experimental scene is displayed after optical correction;
- **Track results**, where the identification results relevant to the robotic fish (position and moving direction) and environmental objects (position) are synchronously displayed;

- **Parameters settings**, in which the user can define color information for robotic fish and environments (goals, obstacles, etc);
- **Individual fish control**, where the user can manually test and check the status of robotic fish, including velocity, direction, adopted mode, etc;
- **Online debugging information**, in which the running status of the system is shown to facilitate the later debugging;
- **Task selection**, where the operator is able to preset, select, and even add different cooperative tasks.
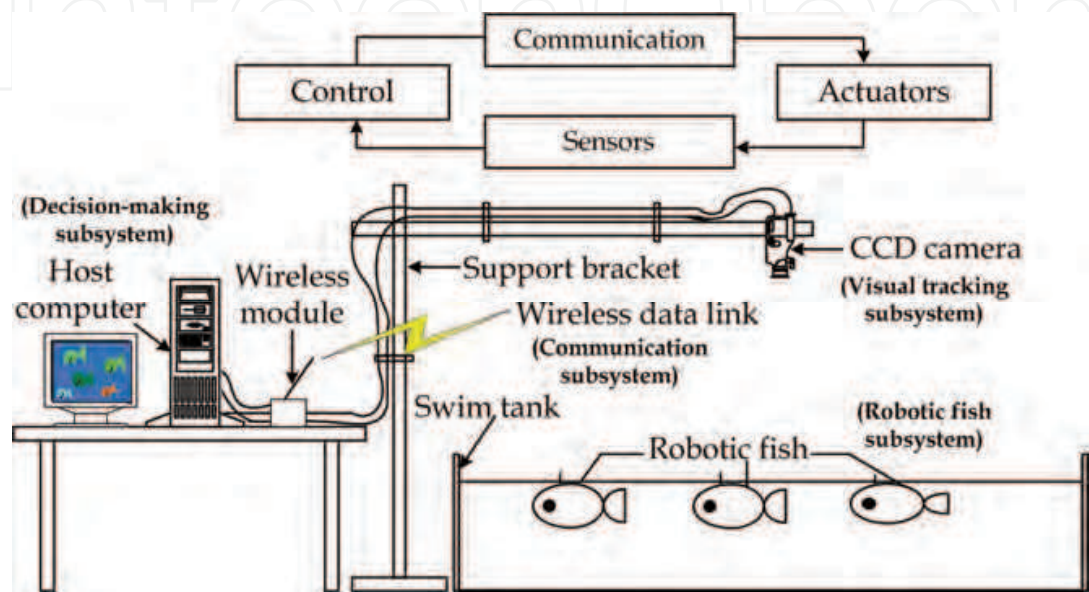
Figure 15. Hardware platform for the MRFS

Figure 16. Graphical user interface of the MRFS

Therefore, the MRFS is competent for a variety of environments (goals, obstacles, etc) and tasks, which provides a standard platform to integrate and examine cooperation algorithms for underwater robots.

6. Experiments and results

In this section, three cooperative tasks including passing hole, Fish versus Man (FVM), and water polo are presented to show how fish cooperate or compete with each other to achieve certain tasks. Relevant control strategies and experimental results are detailed as follows.

6.1 Passing hole
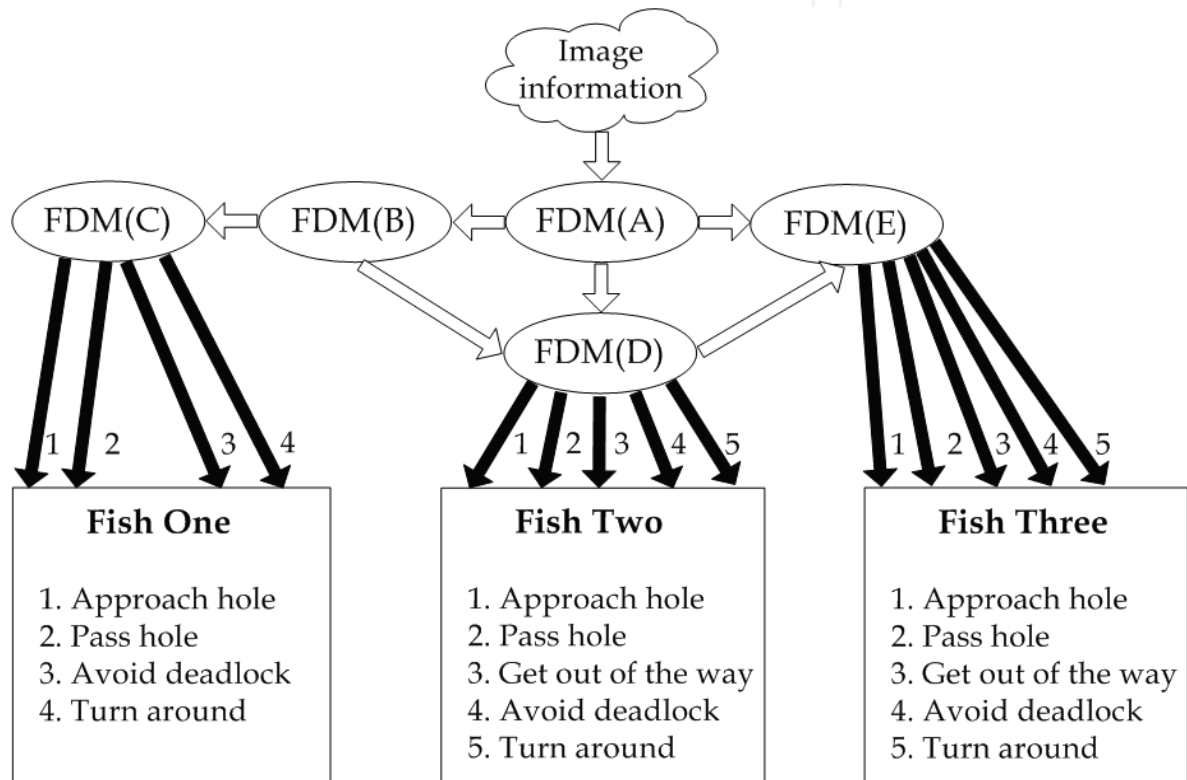
Figure 17. FDM-based behavior architecture for the passing hole. Notice that FDM(A) decides which fish passes the hole now, FDM(B) judges whether other fish should get out of the way, FDM(C) decides which behavior will be taken by Fish One, FDM(D) determines which behavior should be performed by Fish Two and whether Fish Three should get out of the way or not, and FDM(E) selects a suitable behavior for Fish Three

Three fish, in this testing, are required to pass a 150 mm wide hole located in the middle of a water tank according to an appointed order and come back orderly. They also need avoiding collision and mutual crowding during the coordinated motion. Attended roles associating with the appointed passing order, can simply be described as Fish One, Fish Two, and so on. A set of behaviors directed at fast and collision-free swimming are designed as follows:

- **Approach hole**, where the hole is regarded as the goal and the typical PTP algorithm is called.

- **Pass hole**, where the fish adjusts its direction in a small scale when the hole is near. Notice that it will swim straightly at a full speed when the direction is accurate.
- **Avoid deadlock**, where the fish alter its assigned goal to a temporary one in order to get rid of the standstill resulting from insufficient workspace.
- **Turn around**, where some favorable swimming movements are assembled to prepare coming back when a fish has entirely passed the hole. An available alternative is that the fish in full speed stop moving suddenly and turn right or left on a large scale. Thus, the fish can turn around quickly at a very small turning radius.
- **Get out of the way**, where the fish with low priority should get out of the way when obstructing the high-priority one. In particular, this behaviour will work for all fish except Fish One.
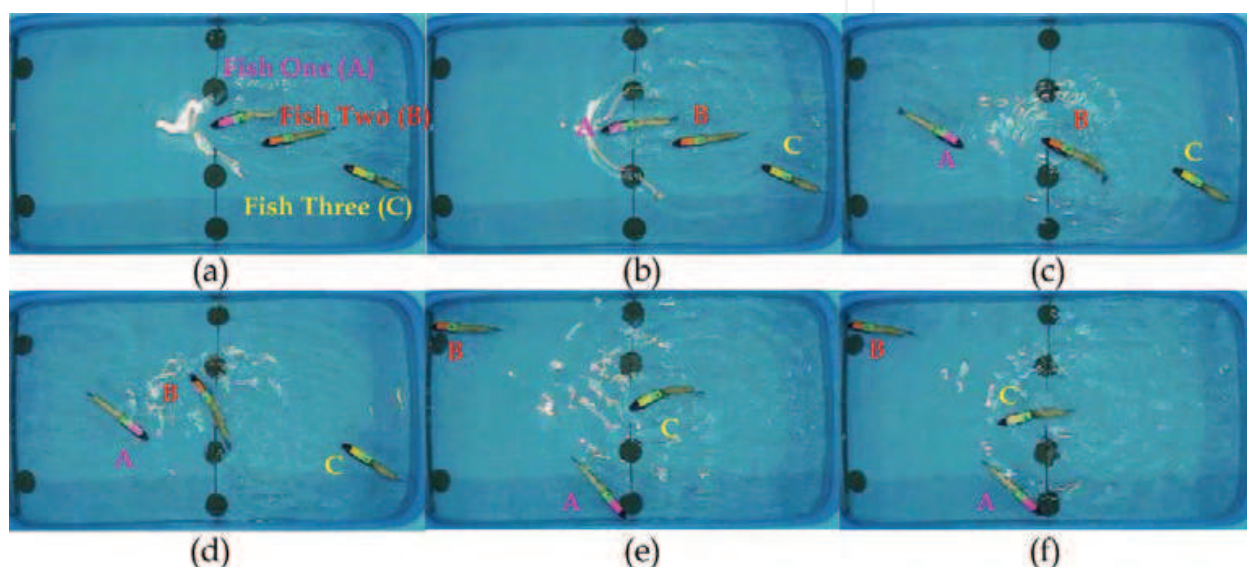
Figure 18. Snapshot sequence of a successful cooperative passing hole [from (a) to (f)]

In order to improve the implementation success rate, a Fuzzy Decision-Making function (FDM) is introduced to coordinate different actions into behaviors, various behaviors into roles, and select suitable roles for different robotic fish. As shown in (9), a FDM has an input variable and two kinds (sometimes only one kind) of output variables.

$$[I_{out}, Be] = \text{FDM}(I_{in}) \tag{9}$$

where I_{in} and I_{out} are the information variables related to the states of fish, environment information, and relative fuzzy rules, and Be is the behavior variable composed of behavior object and action signal. The FDM is based on the minimal "work" criterion, i.e., the sum of the work functions for all selected behaviors and the additive work functions will be minimal. Note that the work function is defined to measure how much work the robotic fish should apply to fulfil the given behaviour, and that the additive work function is also created to coordinate multiple behaviors in terms of fuzzy rules. For instance, if the behaviour X violates any fuzzy rule, it will be set to a large additive work. In contrast to the maximal contribution criterion (Vadakkepat et al., 2004), the minimal work criterion is much easier to perform, since the contribution of a selected behavior is reasonably assessed in an unambiguous fashion. Additionally, the fuzzy rules within this architecture have been translated into functions, i.e., the actions and behaviors coordination are generated via fuzzy

techniques, which are more flexible and easier to operate. Fig. 17 shows the FDM-based behavior architecture for the passing-hole. Therein, the elliptic blocks stand for FDMs and rectangular blocks for sets including executors and optional behaviours. The hollow arrows direct towards only other FDMs, while the solid arrows towards executors and the indexes adjacent to the arrows correspond to the numbered behaviors listed in the rectangular blocks. Notice also that no two behavior variables or information variables can concurrently be generated by a FDM, which avoid any possible conflicts. A successful snapshot for cooperative passing hole is depicted in Fig. 18. As can be observed, there exhibits good coordination among three fish, and the posterior fish will voluntarily give way to the anterior one during going through the narrow hole.

6.2 Fish VS Man

The second cooperation testing is a competitive game between three fish controlled by the computer and a manually controlled fish, called Fish versus Man (FVM). As illustrated in Fig. 19, there exist three goals (about 120 mm wide) in a static pond 3050 mm × 1830 mm × 560 mm (length×width×depth): G_d, G_a, and G_m. Specifically, G_d is the middle goal which divides the field into two section: the left section I is for the three automatic fish denoted as AF and the right part II is occupied by the manually controlled fish which is denoted as MF. G_a and G_m are goals for AF and MF respectively. The rules for this competition are defined as which side first enters into the opponent's goal wins the game. Obviously, one automatic fish can hardly stand against a manually controlled fish. However, when the three members cooperate effectively, the results may be different. Next, we will design the cooperative strategy for the AF team according to the formed hierarchical architecture.
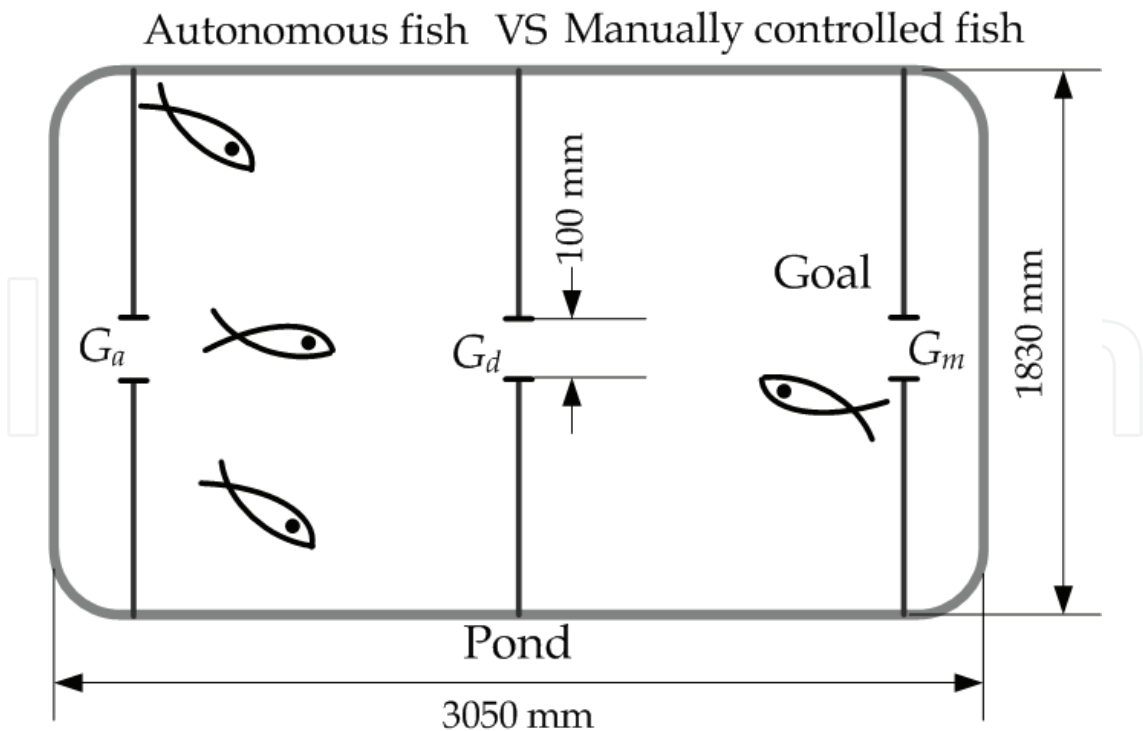

Figure 19. Illustration of the FVM game

The objective for AF team is to swim into G_m as quickly as possible and meanwhile, to prevent MF from intruding G_a. So, achieve this task collectively, the three automatic fish may be divided into three roles: the main attacker who are responsible for swimming to the opponent's goal, the main defense who are responsible for preventing the opposition MF from scoring and buying time for the attacker, and the secondary defense, to assisting the main attacker and blocking the movement of the opponent.

After the roles are produced, we will assign these roles to members of AM in such an order: first, to determine who take on the main defense role, then the secondary defense role, and finally, the attacker. During the assignments, we follow the rules as below.

- The fish nearest to the optimal defending point will be selected as the main defense.
- The one nearest to the optimal secondary defending point becomes the secondary.
- The remainder, naturally, is the attacker. Note that role assignments are dynamic in this case, so the fish may switch between different roles according to progress of the game.

For the attacker, five behaviors are designed as: Go-To-Goal, Avoid-Obstacle, Go-Through-Gate, Stop, and Recovering. For the defenses (both main and secondary), five behaviors are proposed too, which are Get-In-Position, Avoid-Obstacle, Blocking, Stop, and Recovering. Go-To-Goal and Get-In-Position are typical PTP control algorithms presented in Yu et al. (2004). Avoid-Obstacle is to negotiate the nearest obstacle during the movement from the initial position to the destination. Go-Through-Gate behavior allows the fish to pass through the gate in a safe way. Blocking behavior is for the defenses to head the opponent MF off before it approaches G_a. Stop denotes the state without any control input. Recover is the restart behavior, which is employed when the fish has a failure. For each behavior, several actions presented as in Section 2 are organized orderly and executed by setting different parameters to both the speed and the orientation controllers.
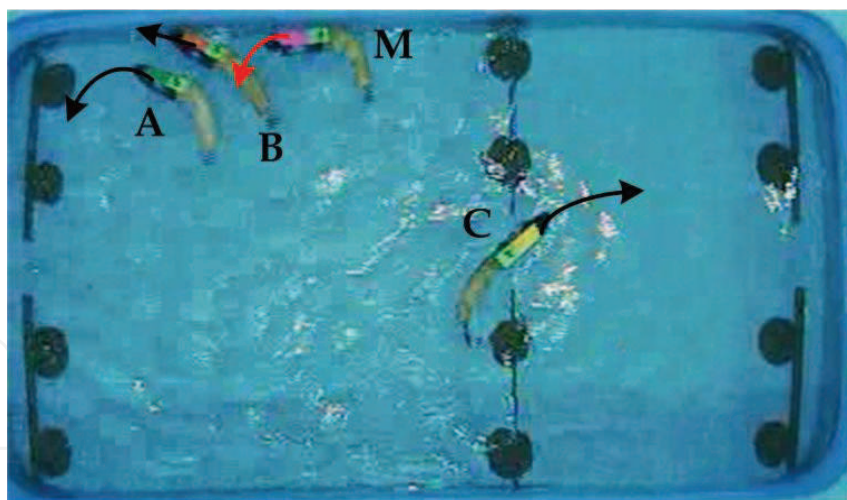

Figure 20. Snapshot of a running FVM game

An experimental snapshot of the game is shown in Fig. 20 and moving trajectories of four robotic fish (A, B, C, and M) in Fig. 21. The three coordinated fish, as we expected, blocked the manually controlled fish successfully and won the game. Clearly, the used coordination strategies worked out. As can be seen from Fig. 21, the scattered points falling into the left-top area of the pond are dense, whereas the points describing the fish C take a figure-eight motion lasting for 25 s. This means the defensive strategies facing the fish M are effective to

some extent, but the Go-Through-Gate behavior usually used the attacker (fish C) are of low efficiency.
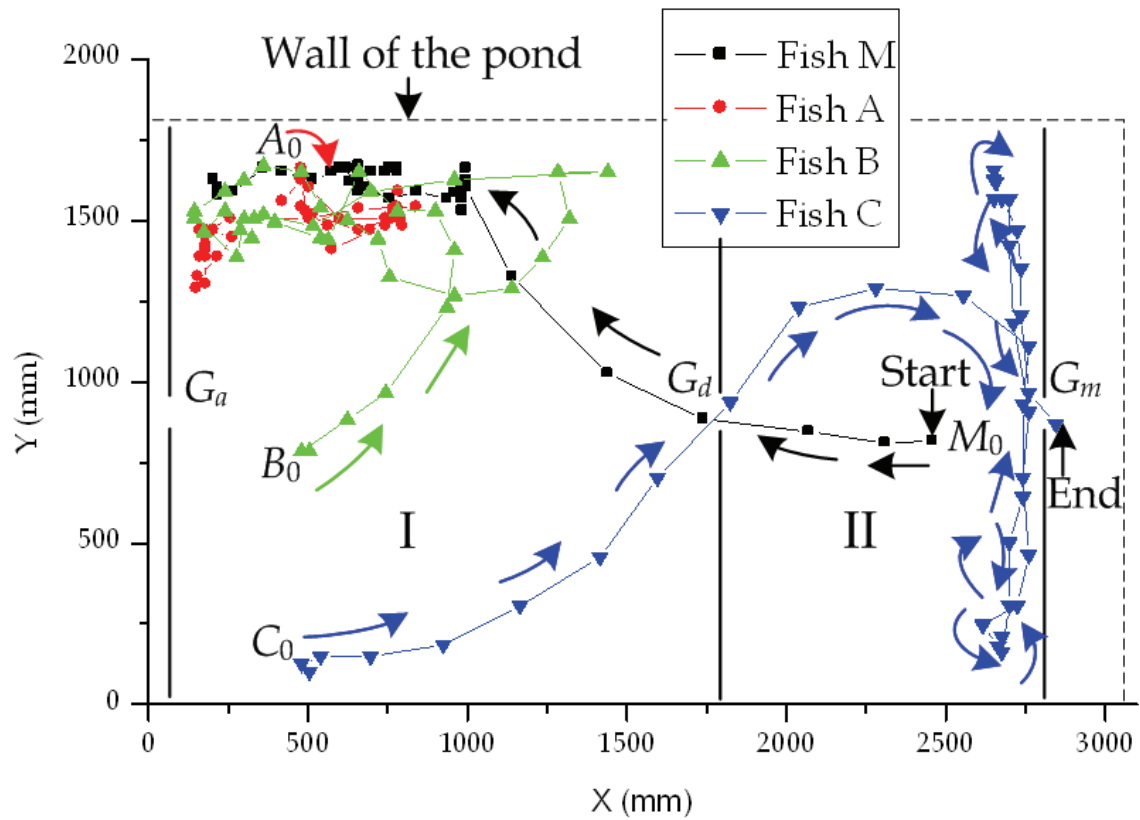

Figure 21. Moving trajectories of the fish in the FVM game lasting 41 s
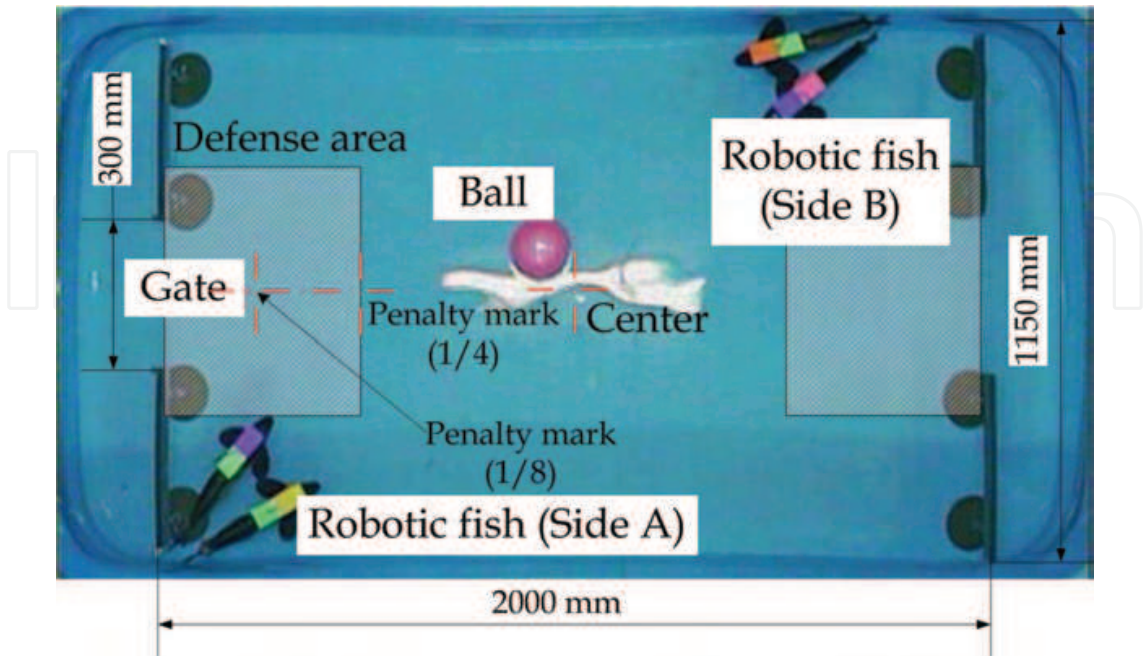
6.3 Water polo

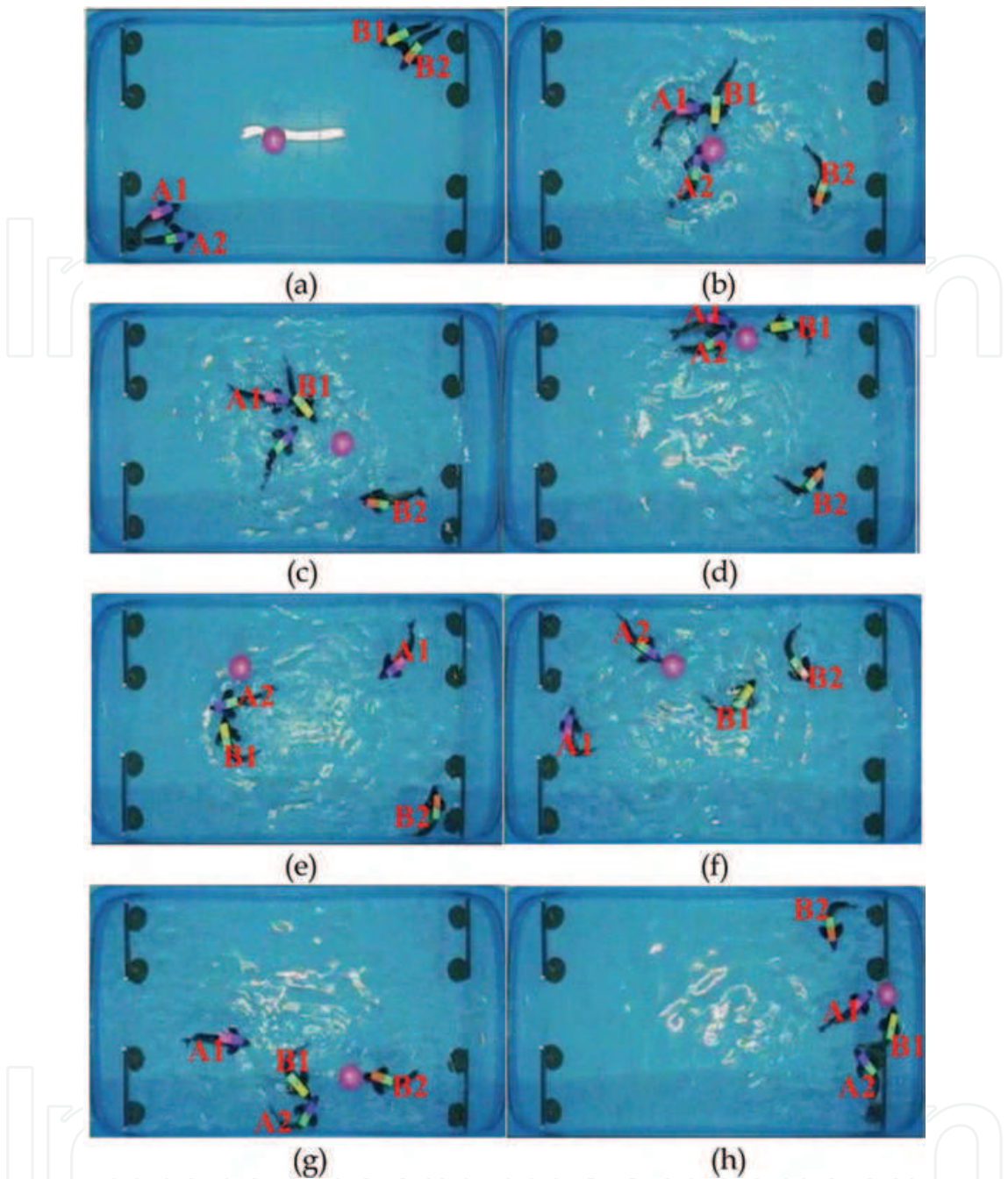Figure 22. Illustration of the water polo

Figure 23. Snapshot sequence of a typical water polo [from (a) to (h)]

The third experiment is designed to let two teams of robotic fish compete with each other through push a polo, which is referred to as "water polo". Similar to the robot soccer game, water polo is intended for providing a standard platform to test and validate aquatic cooperation algorithms. At present, a water polo competition with four robotic fish, i.e., two versus two, is conducted. As shown in Fig. 22, the playground is limited as a water area of 2000 mm × 1150 mm on which four fish grouped as Side A and Side B compete against each other to push the ball to the opponent gate. The rules of the game can be summarized as follows.

- **The robotic fish**. A kind of three-link robotic fish is used as the subject. For convenience of locating robots in motion, two distinguishable color marks are deployed for two sides before the game. Apart from the vision-based color marks, at current stage, no other fish-based sensors are allowed to be mounted for advanced control. In particular, if a robotic fish does not function properly, the game will be paused until a substitution fish in the "second string" enter on the playgroup. Notice that the robotic fish may not be substituted at will and that only three chances of replacements are permitted in a game.
- **The playground**. As shown in Fig. 22, a specific defense area is situated at each end of the water tank. Also penalty marks are set to 1/4 and 1/8 of the longitudinal midline. A pink, 2/3 submerged, inflatable ball is served in the center or penalty mark when starting the water polo. Like the robotic fish, the ball may not be substituted at will unless it becomes defective.
- **The method of scoring.** Like football games, a goal will be scored when the center of the ball gets across the gate baseline. As a rule, the side scoring the greater number of goals in a game is the winner.
- **The duration of game.** The game lasting 30 minutes is divided into two equal playing periods for the moment.

Fig. 23 depicts an image sequence of a running water polo, in which two teams Side A and Side B take different strategies: in Side A, both robotic fish are attackers, whereas in Side B, B1 is an attacker and B2 is a defense. Finally A1 hits the ball into the opponent gate and hence Side A makes a point. We remark that the game water polo emphasizes the strategy, and different strategies may lead to different results. Here, we only adopt one possible strategy, and other choices should be further examined and verified.

6.4 Discussions

Extensive experiments have been carried out to verify the feasibility and effectiveness of the formulated cooperative framework and adopted strategies. However, the experimental results for the moment are not perfect but successful and promising, which are mainly affected by the following unsolved or open factors.

- **Controllability**. This factor involves the controllability of both the fish-like robots and the behavioral framework. For the former, fish-like swimming skills and intelligence can not be fully mimicked. The necessities of high swimming skills include hydrodynamic based modeling and sensors based perception. Unfortunately, dynamic models, smart sensors, communication links, as well as on-board processing integrated control algorithms, are still not well tackled in underwater environments and in fish-like robots. This deficiency will debase the capability of swimming and further impact the performance of the collective behaviors to a large extent. For the latter, how to avoid conflicts and ensure operational efficiency is the key to fulfil high-quality cooperative control since the behavioral framework do not directly define an input-output structure.
- **Uncertainty.** There are two uncertainties that constrain the repeatability of the applied control strategies. One is from the measurement error of the vision subsystem due to changing lighting and splashed waves. This would bring trouble in performing precise motion control. Another source is the manufacture of the robotic fish. Because the

robots are made manually, there exists small performance difference among the developed robots, such as the maximum speed and minimum turning radius, etc.

- **Scalability.** Because of the restriction of the experiment field, to avoid mutual collision frequently and to improve operational efficiency, there is an upper limit on the fish number participating in the cooperation. When a larger space is available, more fish will swim freely in the pond, and other complicated tasks such as self-organized schooling and cooperative formation control may be designed, but in turn complicating the control laws design.

- **Compatibility.** The conceived cooperative experiments are performed in the indoor environment. Especially, the global vision subsystem prohibits the widespread use of the MRFS in complex outdoor environments. To achieve real autonomy, some fish-based sensors and processors should be imported. In addition, the MFRS only handles 2-D swimming behaviors. Since vivo fish gracefully execute maneuvers with ease in 3-D aquatic environments, design and implementation of robotic fish enabling 3-D movements are highly needed to future real-world applications. Of course, the current behaviour cooperation architecture can also be applied to 3-D hydrodynamic environments but requires some further adaptations so that it becomes a part of the admissible, 3-D swimming-oriented system behaviors.

7. Conclusion

This chapter has reviewed some of the issues involved in creating a multiple robotic fish cooperation platform inspired by the astonishing cooperative power exhibited by fish school. Grounded on an optimized kinematic and dynamic model of robotic fish, a group of radio-controlled, multi-link fish-like robots as well as their motion control were developed. To enable a closed control loop, a vision-based multi-object tracking subsystem for multiple robotic fish was built, where an improved parallel visual tracking method is formulated within a framework synthesizing features of fish features and surrounding disturbance. A hierarchical architecture for the artificial multi-fish system was further proposed to generate coordinated behaviours and actions. Experimental results on three typical cooperation tasks demonstrated the effectiveness of the proposed scheme.

The ongoing and future work will focus on developing a 3-D dynamic model for free-swimming, multi-link robots and on investigating experimentally the corresponding control laws, which makes preparations for cooperative control of multiple robotic fish in 3-D aquatic environments. In addition, some learning algorithms will be incorporated into the cooperative framework to enhance the cooperation efficiency.

8. Acknowledgement

9. References

Anderson, J.M. & Chhabra, N.K. (2002). Maneuvering and stability performance of a robotic tuna, *Integ. and Comp. Biol.*, Vol. 42, 2002, pp. 118–126

Bandyopadhyay, P.R. (2004). Guest editorial: Biology-inspired science and technology for autonomous underwater vehicles, *IEEE J. Ocean. Eng.*, Vol. 29, No. 3, Jul. 2004, pp. 542–546

Bandyopadhyay, P.R. (2005). Trends in biorobotic autonomous undersea vehicles, *IEEE J. Ocean. Eng.*, Vol. 30, No. 1, 2005, pp. 109–139

Barrett, D.S. (1996). Propulsive efficiency of a flexible hull underwater vehicle, *Dissertation for the Doctoral Degree*, Cambridge, MA: Massachusetts Institute of Technology

Das, A.K.; Fierro, R.; Kumar, V.; Ostrowski, J.P.; Spletzer, J. & Taylor, C.J. (2002). A vision-based formation control framework, *IEEE Transactions on Robotics and Automation*, Vol. 18, No. 5, October 2002, pp. 813–825

Kumar, V. ; Leonard, N. & Morse, A. S. (Eds.) (2005). *Cooperative Control*, *Lecture Notes in Control and Information Sciences*, Vol. 309, Berlin: Springer-Verlag

Lauder, G.V. ; Anderson, E.J.; Tangorra, T.J. & Madden, P.G.A. (2007a). Fish biorobotics: kinematics and hydrodynamics of self-propulsion, *The Journal of Experimental Biology*, Vol. 210, 2007, pp. 2767–2780

Lauder, G.V. & Madden, P.G.A. (2007b). Fish locomotion: kinematics and hydrodynamics of flexible foil-like fins, *Exp. Fluids*, Vol. 43, 2007, pp. 641–653

Ögren, P. ; Fiorelli, E. & Leonard, N.E. (2004). Cooperative control of mobile sensor networks: adaptive gradient climbing in a distributed environment, *IEEE Transactions on Automatic Control*, Vol. 49, No. 8, August 2004, pp. 1292–1302

Pettersen, K.Y. ; Gravdahl, J.T. & Nijmeijer, H. (Eds.) (2006). *Group Coordination and Cooperative Control*, *Lecture Notes in Control and Information Sciences*, Vol. 336, Berlin: Springer-Verlag

Rabbath, C.A. ; Su, C.Y. & Tsourdos, A. (2007). Guest editorial: introduction to the special issue on multivehicle systems cooperative control with application, *IEEE Transactions on Control System Technology*, Vol. 15, No. 4, July 2007, pp. 599–600

Read, D.A.; Hover, F.S. & Triantafyllou, M.S. (2003). Forces on oscillating foils for propulsion and maneuvering, *J. Fluids and Structure*, Vol. 17, 2003, pp. 163–183

Sfakiotakis, M.; Lane, D.M. & Davies, J.B.C. (1999). Review of fish swimming modes for aquatic locomotion, *IEEE J. Oceanic Eng.*, Vol. 24, No. 2, Apr. 1999, pp. 237–252

Triantafyllou, M.S. & Triantafyllou, G.S. (1995). An efficient swimming machine, *Sci. Amer.*, Vol. 272, No. 3, March 1995, pp. 64–70

Triantafillou, M.S.; Techet, A.H. & Hover, F.S. (2004). Review of experimental work in biomimetic foils, *IEEE J. Ocean. Eng.*, Vol. 29, No. 3, 2004, pp. 585–594

Yu, J.; Tan, M. & Wang, S. (2003). A parallel algorithm for visual tracking of multiple free-swimming robot fishes based on color information, *Proc. IEEE Int. Conf. Robot., Intelligent Syst. Signal Process*, 2003, pp. 359–364, Changsha, China

Yu, J.; Tan, M.; Wang, S. & Chen, E. (2004). Development of a biomimetic robotic fish and its control algorithm, *IEEE Trans. Syst., Man, Cybern. B, Cybern.*, Vol. 34, No. 4, July 2004, pp. 1798–1810

Yu, J.; Wang, L. & Tan, M. (2005). A framework for biomimetic robot fish's design and its realization, *Proc. Amer. Contr. Conf.*, 2005, pp. 1593–1598, Port-land, OR, USA

Yu, J.; Liu, L. & Wang, L. (2006a). Dynamics and control of turning maneuver for biomimetic robotic fish, *Proc. of IEEE/RSJ International Conference on Intelligent Robots and Systems*, pp. 5400–5405, October 2006, Beijing, China

Yu, J.; Fang, Y.; Wang, L. & Liu, L. (2006b). Visual tracking of multiple robotic fish for cooperative control, *Proc. of IEEE International Conference on Robotics and Biomimetics (ROBIO 2006)*, pp. 85–90, Kunming, China, Dec. 2006

Yu, J.; Wang, L. & Tan, M. (2007). Geometric optimization of relative link lengths for biomimetic robotic fish, *IEEE Trans. Robot.*, Vol. 23, No. 2, 2007, pp. 382–386

Videler, J.J. & Hess, F. (1984). Fast continuous swimming of two pelagic predators, saithe (Pollachius virens) and mackerel (Scomber scombrus): a kinematic analysis. *J. Exp. Biol.*, Vol. 109, 1984, pp. 209–228

Vadakkepat, P.; Miin, O. C.; Peng, X. & Lee, T.H. (2004). Fuzzy behavior-based control of mobile robots, *IEEE Transactions on Fuzzy Systems*, Vol. 12, No. 4, 2004, pp. 559–564

Wang, X. ; Yadav, V. & Balakrishnan, S. N. (2007). Cooperative UAV formation flying with obstacle/collision avoidance, *IEEE Transactions on Control System Technology*, Vol. 15, No. 4, July 2007, pp. 672–679

Zhang, D.; Wang, L. & Yu, J. (2007). Coordinated transport by multiple biomimetic robotic fish in underwater environment, *IEEE Transactions on Control System Technology*, Vol. 15, No. 4, July 2007, pp. 658–671

Recent Advances in Multi Robot Systems

Edited by Aleksandar Lazinica

To design a team of robots which is able to perform given tasks is a great concern of many members of robotics community. There are many problems left to be solved in order to have the fully functional robot team. Robotics community is trying hard to solve such problems (navigation, task allocation, communication, adaptation, control, ...). This book represents the contributions of the top researchers in this field and will serve as a valuable tool for professionals in this interdisciplinary field. It is focused on the challenging issues of team architectures, vehicle learning and adaptation, heterogeneous group control and cooperation, task selection, dynamic autonomy, mixed initiative, and human and robot team interaction. The book consists of 16 chapters introducing both basic research and advanced developments. Topics covered include kinematics, dynamic analysis, accuracy, optimization design, modelling, simulation and control of multi robot systems.

INTECH
open science | open minds